International Journal on Magnetic Particle Imaging
Vol 9, No 1, Suppl 1, Article ID 2303013, 4 Pages

Infinite Science Publishing

Proceedings Article

Characterization of magnetic targeting effectivity in an artificial tumor vessel network

Lukas Glänzer[a] · Max C. Lindemann[a] · Benedikt Mues[a] · Klaus Kreuels[b] · Nadine Nottrodt[b] · Thomas Schmitz-Rhode[a] · Ioana Slabu[a,*]

[a]Applied Medical Engineering, RWTH Aachen University, Aachen, Germany
[b]Fraunhofer Institute for Laser Technology, RWTH Aachen University, Aachen, Germany
*Corresponding author, email: slabu@ame.rwth-aachen.de

Abstract

Magnetic nanoparticles (MNP) can be used as drug carriers in novel cancer treatment approaches such as magnetic drug targeting (MDT). Computer simulations of MNP in a tumor vessel network under the influence of a magnetic field considering the physical and chemical properties of MNP were established before, however, an experimental validation of these simulations for specific settings is missing. The parameters influencing the targeting effectivity such as MNP concentration, blood flow velocities and different distances of the tumor vessel network to the magnet configuration were varied and a quantitative assessment of the targeting effectivity was performed photometrically determining the resulting iron concentration. Magnetic particle imaging (MPI) was used to analyze the correlation between MPI intensity values and the iron concentration. The parameter study confirmed the previous simulation results for the fixed magnet configuration.

I. Introduction

Magnetic drug targeting (MDT) describes the selective targeting of therapeutics in a tissue or a region in the body, e. g. in a tumor, by an external magnetic field to allow a controlled drug release. Lindemann et al. [1] created a FEM based simulation to understand the relevant MDT properties in a multibranched vessel network to achieve a higher targeting effectivity.

The aim of this study is the design of a reproducible experimental setup to characterize the magnetic targeting effectivity. For this, an 8-branched artificial tumor vessel network (ATVN) [2, 3] was 3D-printed at the ILT of the RWTH Aachen University. To conduct reproducible experiments with clear positioning of the components (base plate, support structure and magnet adapter), a fixture for the ATVN and the magnetic trap was designed. A parameter study of the targeting effectivity for different concentrations, velocities and magnet distances was performed. The experiments are evaluated by photometrically determining the iron concentration. Also, magnetic particle imaging (MPI) was used to measure setups of different concentration to analyze the correlation between the MPI intensity values and the setups' iron concentration.

II. Material and methods

The ferrofluid used was a suspension of magnetite-MNP in distilled water as the carrier fluid. The magnetite core of the MNP had an average diameter of $d_c = (10.2 \pm 2.4)$ nm. The superparamagnetic MNP exhibited a saturation magnetization of $M_s = (99.4 \pm 0.8)\,\mathrm{A\,m^2\,kg^{-1}}$ [4].

MPI measurements were performed using a commercial imaging system (MPI 25/20 FF, Bruker BioSpin

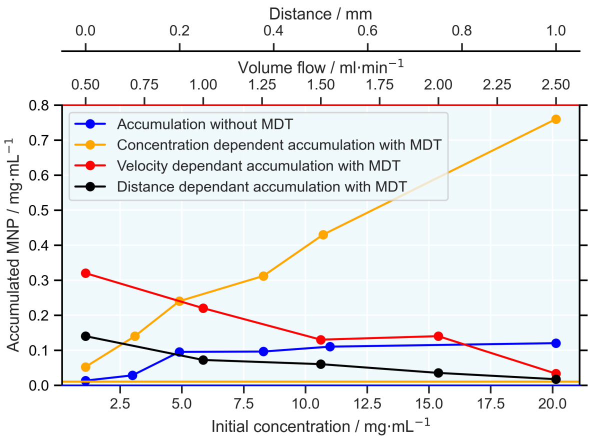

Figure 1: Total amount of accumulated MNP measured for the different setups and the reference value.

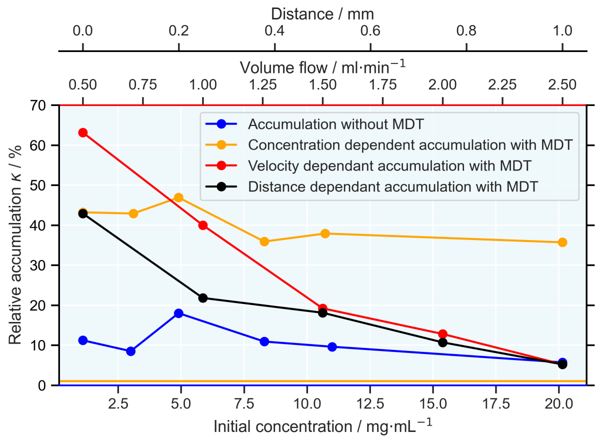

Figure 2: Relative amount of accumulated MNP measured for the different setups and the reference value.

MRIGmbH, Ettlingen, Germany).

For photometric determination of the iron concentrations, the complexion of Fe-$^{3+}$ with 4.5-Dihydroxy-1.3-benzoldisulfon acid disodium salt hydrate (tiron) was used. This solution characteristically absorbs light at $\lambda = 480\,\text{nm}$, thus the absorbance value can be measured and is linearly dependent on the MNP concentration.

The fixture for the ATVN consisting of a base plate, a support structure and a magnet adapter was 3D-printed (Veroclear RGD 450).

III. Results and discussion

For the study, the iron concentrations, the volume flow of the ferrofluid and the distance of the magnets to the ATVN were varied. As reference, an experiment without applying an external magnetic field was conducted to determine the MNP accumulation in the ATVN geometry. For this, a constant volume flow of 1 $\text{ml}\,\text{min}^{-1}$ was used. MPI measurements were used to acquire a calibration curve to quantify the setups' iron concentration.

III.I. Photometric evaluation

For the concentration variations, the accumulation caused by the geometry increases slowly and reaches a plateau at a concentration of 12 $\text{mg}\,\text{ml}^{-1}$ (Fig 1, blue line). The targeted accumulation has a linear increase with increasing concentration (Fig 1, orange line). Regarding the concentration, the highest relative accumulation can be detected at 4.9 $\text{mg}\,\text{ml}^{-1}$ (Fig 2, orange line).

The volume flow variations were conducted with an concentration of 4.9 $\text{mg}\,\text{ml}^{-1}$ and 0 mm distance between the magnet configuration and the test tube. As the MNP drag of the blood flow acts directly against the magnetic force [5], the accumulation decreases with increasing volume flow. Consequently, the highest total accumulation (Fig 1, red line) and the highest relative accumulation (Fig 2, red line) was measured at 0.5 $\text{ml}\,\text{min}^{-1}$.

The distance variations were conducted with an concentration of 3 $\text{mg}\,\text{ml}^{-1}$ and a volume flow of 1 $\text{ml}\,\text{min}^{-1}$. An increasing distance between the magnet configuration and the ATVN has a decreasing effect on the accumulated MNP. As expected, the highest total accumulation (Fig 1, black line) and the highest relative accumulation (Fig 2, black line) were measured at 0 mm distance. This implies, that deep seated tumors are hardly targetable in vivo with the magnet configuration outside the body. However, hollow organs can be reached by insertion via an endoscope [6, 7]. At their respective concentrations, the relative accumulation κ in the volume flow variations and in the distance variation are lower than the accumulation of the reference values, i.e., for the volume flow dependency $\kappa_{\text{velocity,min}} = 5.2\%$ whereas $\kappa_{\text{reference},c=4.9} = 18.3\%$ and for the distance dependency $\kappa_{\text{distance,min}} = 5.2\%$ whereas $\kappa_{\text{reference},c=3} = 8.5\%$. An explanation could be the fact that depending on the magnet cofiguration MNP are pushed from the vessel wall into the middle of the vessel, where they experience a strong drag with the blood flow. This has a negative effect on targeting effectivity [1]. With greater volume flow the effect of the magnetic force decreases. Further, the MNP accumulated at the bifurcation of the channels experience a significantly higher force on impact, resulting in a lower possibility of accumulation.
The maximum relative accumulation is at $\kappa_{\text{velocity,max}} = 63.14\%$. As the maximum relative accumulation of the reference setup is at 18.3%, the highest percentile which is achieved exclusively through magnetic targeting is at 44.84 %. Thus, the setup with highest relative accumulation is found at a concentration of 4.9 $\text{mg}\,\text{ml}^{-1}$, a volume flow of 0.5 $\text{ml}\,\text{min}^{-1}$ and a 0 mm distance.

10.18416/ijmpi.2023.2303013

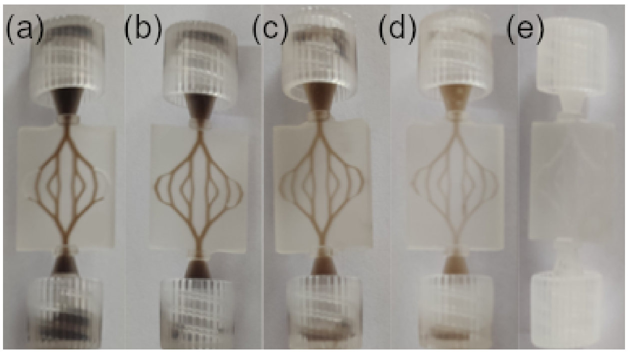

Figure 3: Experimental setups for calibration with different MNP concentrations. (a) 1 mg ml^{-1} (b) 0.75 mg ml^{-1} (c) 0.5 mg ml^{-1} (d) 0.2 mg ml^{-1} (e) 0 mg ml^{-1}

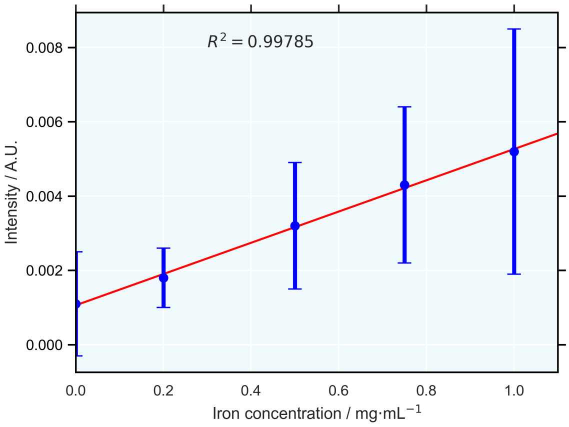

Figure 4: Linearly fitted intensities from MPI measurements of the calibration setups.

III.II. MPI Evaluation

To acquire a calibration curve, setups with different MNP concentrations were measured with the MPI (Fig 3). The results were evaluated by analyzing the intensities returned by the MPI. The measured intensities are plotted against the known iron concentrations (Fig 4) and linearly fitted. The fit indicates a very clear linear dependency ($R^2 = 0.99785$) between the iron concentration and the intensity value. Whether this dependency holds for higher or lower concentrations needs to be tested in further studies.
These results confirm the validity of the FEM simulations by Lindemann et al. [1]. The magnet configuration has a significant effect on the targeting effectivity. By increasing the number of magnets, the configuration yields a large number of magnetic field maxima that are approached with a high gradient. Thus, future studies need to investigate the influence of different magnet configurations on the targeting effectivity. Additionally, the linear dependency between the iron concentration and the MPI intensity value needs to be validated.

IV. Conclusion

In this work, an experimental validation of established computer simulations was performed to investigate the targeting effectivity of MNP with an ATVN as the targeting region. The resulting MNP concentrations were measured with respect to the concentration, the volume flow and the magnet distance to the ATVN. The results show a clear increase of the MNP accumulation with increasing concentration applied into the setup. The relative MNP accumulation value indicates a maximum of the relative accumulation at an concentration of $c_{MNP} = 4.9\,\mathrm{mg\,ml^{-1}}$. When increasing the volume flow, the targeted concentration decreases significantly. For a distance of $s_f > 0.75\,\mathrm{mm}$ the relative accumulation value drops below the reference value, resulting in no effect of the MDT. This shows that the externally applied magnets must be in close distance to the targeted region.

Acknowledgments

We thank the Institute for Experimental Molecular Imaging at the RWTH Aachen University for providing access to the MPI device. We also thank Jan Marshall for helping with conducting the experiments. This research is funded by the DFG Grant No. 467959793 and the START-Research Funding of the UKA Grant No. 118/21.

Author's statement

Conflict of interest: Authors state no conflict of interest.

References

[1] M. C. Lindemann, T. Luttke, N. Nottrodt, T. Schmitz-Rode, and I. Slabu. Fem based simulation of magnetic drug targeting in a multibranched vessel model. *Computer Methods and Programs in Biomedicine*, 210:106354, 2021.

[2] X. Han, J. Courseaus, J. Khamassi, N. Nottrodt, S. Engelhardt, F. Jacobsen, C. Bierwisch, W. Meyer, T. Walter, J. Weisser, R. Jaeger, R. Bibb, and R. Harris. Optimized vascular network by stereolithography for tissue engineered skin. *International Journal of Bioprinting*, 4(2), 2018.

[3] R. Bibb, N. Nottrodt, and A. Gillner. Artificial vascularized scaffolds for 3d-tissue regeneration — a report of the artivasc 3d project. *International Journal of Bioprinting*, 2(1), 2016.

[4] B. Mues, E. M. Buhl, T. Schmitz-Rode, and I. Slabu. Towards optimized mri contrast agents for implant engineering: Clustering and immobilization effects of magnetic nanoparticles. *Journal of Magnetism and Magnetic Materials*, 471:432–438, 2019, doi:https://doi.org/10.1016/j.jmmm.2018.09.119.

[5] P. Cregg, K. Murphy, and A. Mardinoglu. Calculation of nanoparticle capture efficiency in magnetic drug targeting. *Journal of Magnetism and Magnetic Materials*, 320(23):3272–3275, 2008.

[6] A. A. Roeth, I. Garretson, M. Beltz, T. Herbold, M. Schulze-Hagen, S. Quaisser, A. Georgens, D. Reith, I. Slabu, C. D. Klink, *et al.* 3d-printed replica and porcine explants for pre-clinical optimization of endoscopic tumor treatment by magnetic targeting. *Cancers*, 13(21):5496, 2021.

[7] A. A. Roeth, I. Slabu, M. Baumann, P. H. Alizai, M. Schmeding, G. Guentherodt, T. Schmitz-Rode, and U. P. Neumann. Establishment of a biophysical model to optimize endoscopic targeting of magnetic nanoparticles for cancer treatment. *International journal of nanomedicine*, 12:5933, 2017.

10.18416/ijmpi.2023.2303013